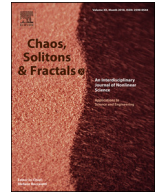




Contents lists available at ScienceDirect

# Chaos, Solitons and Fractals

Nonlinear Science, and Nonequilibrium and Complex Phenomena

journal homepage: [www.elsevier.com/locate/chaos](http://www.elsevier.com/locate/chaos)

## Embedded solitons in second-harmonic-generating lattices

Hadi Susanto<sup>a,b,\*</sup>, Boris A. Malomed<sup>c,d</sup><sup>a</sup> Department of Mathematics, Khalifa University, Abu Dhabi Campus, PO Box 127788, Abu Dhabi, United Arab Emirates<sup>b</sup> Department of Mathematical Sciences, University of Essex, Wivenhoe Park, Colchester CO4 3SQ, United Kingdom<sup>c</sup> Department of Physical Electronics, School of Electrical Engineering, Faculty of Engineering, and Center for Light-Matter Interaction, Tel Aviv University, Tel Aviv 69978, Israel<sup>d</sup> Instituto de Alta Investigación, Universidad de Tarapacá, Casilla 7D, Arica, Chile

### ARTICLE INFO

#### Article history:

Received 14 November 2020

Accepted 1 December 2020

#### Keywords:

Embedded soliton

Discrete soliton

Variational approximation

### ABSTRACT

Embedded solitons are exceptional modes in nonlinear-wave systems with the propagation constant falling in the system's propagation band. An especially challenging topic is seeking for such modes in nonlinear dynamical lattices (discrete systems). We address this problem for a system of coupled discrete equations modeling the light propagation in an array of tunnel-coupled waveguides with a combination of intrinsic quadratic (second-harmonic-generating) and cubic nonlinearities. Solutions for discrete embedded solitons (DESs) are constructed by means of two analytical approximations, adjusted, severally, for broad and narrow DESs, and in a systematic form with the help of numerical calculations. DESs of several types, including ones with identical and opposite signs of their fundamental-frequency and second-harmonic components, are produced. In the most relevant case of narrow DESs, the analytical approximation produces very accurate results, in comparison with the numerical findings. In this case, the DES branch extends from the propagation band into a semi-infinite gap as a family of regular discrete solitons. The study of stability of DESs demonstrates that, in addition to ones featuring the well-known property of semi-stability, there are linearly stable DESs which are genuinely robust modes.

© 2020 Elsevier Ltd. All rights reserved.

### 1. Introduction

One of basic scenarios of nonlinear optics is the generation of second-harmonic (SH) waves by the fundamental-frequency (FF) input in waveguides with a quadratic, alias  $\chi^{(2)}$ , material response [1]. The interplay of the  $\chi^{(2)}$  nonlinearity with linear paraxial diffraction of light in planar waveguides gives rise to spatial solitons of the  $\chi^{(2)}$  type, which are built of quadratically coupled FF and SH components. Such solitons were first predicted as particular exact solutions of a system of two coupled equations for the paraxial propagation of amplitudes of the FF and SH waves [2], and later created experimentally [3]. Theoretical and experimental studies of  $\chi^{(2)}$  solitons have grown into a vast research area [4–6].

Varieties of  $\chi^{(2)}$  dynamical effects and, in particular, soliton modes, are additionally expanded in settings which combine quadratic and cubic ( $\chi^{(3)}$ ) terms [7,8]. There are two distinct types of such combinations: competing, if the  $\chi^{(3)}$  term is self-defocusing, and cooperating, if the latter term has the focusing sign. One of specific phenomena predicted in models with the

combined  $\chi^{(2)} : \chi^{(3)}$  nonlinearity is the existence of *embedded solitons* [9] i.e., localized modes whose propagation constant, rather than belonging, as usual, to spectral gaps, in which the propagation of linear waves is suppressed by the system's dispersion relation, falls (is *embedded*) in a propagation band. Normally, solitons cannot exist in such a case, as the resonance between propagation constants of the solitons and linear waves gives rise to decay of the (quasi-) soliton modes into radiation. Nevertheless, in exceptional cases, i.e., at some isolated values of the soliton's propagation constant, the decay rate may vanish (in other words, the resonance strength becomes exactly equal to zero), which explains the existence of embedded solitons. This possibility was originally proposed in Refs. [10] and [11] (without naming such modes “embedded” ones), see an early review of the topic in Ref. [12]. In the linear version of the  $\chi^{(2)}$  system, dispersion relations for the FF and SH waves are decoupled, each consisting of a semi-infinite propagation band and forbidden gap. Boundaries between the gap and band in the FF and SH spectra are mutually shifted, in the general case, due to the mismatch between the FF and SH components. In terms of the FF wave, the propagation constant of any soliton must always belong to the respective gap. However, the SH propagation equation, with the SH amplitude driven by the square of the FF, may have *nonlinearizable* solutions. For such states, the quadratic

\* Corresponding author at: Department of Mathematics, Khalifa University, Abu Dhabi Campus, PO Box 127788, Abu Dhabi, United Arab Emirates.

E-mail address: [hadi.susanto@ku.ac.ae](mailto:hadi.susanto@ku.ac.ae) (H. Susanto).

(FF  $\times$  FF) term in the SH equation cannot be omitted when considering exponentially decaying tails of the soliton's fields, as it has the same order of magnitude as linear SH terms ("tail-locked" modes) [9]. Thus, the SH propagation constant of these solutions does not need to obey the spectral structure of the linearized equation, falling, counter-intuitively, into the propagation band for the SH component.

Because, as mentioned above, embedded solitons exist only at specially selected value(s) of the propagation constant, they do not form continuous families, being categorized, accordingly, as *codimension-one* solutions (see, e.g. Ref. [13]). Another specific feature of embedded solitons is their (in)stability. In most cases, they are neutrally stable against small perturbations in the linear approximation, but are unstable against the (slower-than-exponential) growth of perturbations driven by terms which are quadratic, with respect to the small perturbations [9]. In some cases, such "semi-stable" solitons may seem as practically stable ones, if the nonlinear growth of the perturbations is extremely slow [12], and there are particular models which support completely stable embedded solitons [14].

One of ramifications of studies of  $\chi^{(2)}$  solitons is the creation of their discrete counterparts in arrays (lattices) of tunnel-coupled waveguides with the quadratic or combined quadratic-cubic intrinsic nonlinearities in individual guiding cores [15,16]. A challenging possibility is to search for discrete embedded solitons (DEs) in the respective system of lattice-propagation equations for amplitudes of the FF and SH waves, coupled by the quadratic nonlinearity acting at lattice sites. This objective was a subject of Ref. [17]. In that work, only a partial consideration of the problem was performed; in particular, only DEs with opposite signs of the FF and SH components were found. Note that no analytical methods were applied in Ref. [17]. In the present work, we aim to develop the consideration of DEs in  $\chi^{(2)}$  lattices, elaborating an analytical approximation (the averaging method), in parallel to producing systematic numerical results, and producing DEs of more general types, featuring both identical and opposite signs of the FF and SH components. Additionally, we also consider stability of the DEs.

The model is formulated in Section 2, and two analytical methods are presented in Section 3. One of them (the quasi-continuum approximation) is relevant for broad DEs, and the opposite anti-continuum approximation, applies, with high accuracy, to strongly discrete solitons. Numerical results are reported, and compared to the analytical approximations, in Section 4. Stability of DEs is investigated in the same section by means of computing eigenvalues of the linearisation operator and direct simulations of the perturbed evolution. We also report the existence of linearly stable embedded solitons in the weakly coupled lattice. The paper is completed by Section 5.

## 2. The model

We start with the discrete one-dimensional system with the on-site  $\chi^{(2)}$  :  $\chi^{(3)}$  nonlinearity, which was introduced in Ref. [17]:

$$i \frac{du_n}{dz} + \epsilon \Delta u_n + u_n^* v_n + \gamma_1 (|u_n|^2 + 2|v_n|^2) u_n = 0, \quad (1a)$$

$$i \frac{dv_n}{dz} - \epsilon \delta \Delta v_n + q v_n + \frac{1}{2} u_n^2 + 2\gamma_2 (|v_n|^2 + 2|u_n|^2) v_n = 0. \quad (1b)$$

Here  $\epsilon$  is the coefficient of coupling between adjacent sites of the underlying lattice for complex amplitude  $u_n$  of the FF wave,  $\delta \geq 0$  is the relative lattice-coupling coefficient for amplitude  $v_n$  of the SH wave, the finite-difference Laplacian is  $\Delta X_n = X_{n+1} + X_{n-1} - 2X_n$ , the SH-FF mismatch is accounted for by constant  $q$ , the coefficient of the  $\chi^{(2)}$  interaction is scaled to be 1, and  $\gamma_{1,2}$  are coefficients of the  $\chi^{(3)}$  self-interaction for the FF and SH waves. All

coefficients in Eqs. (1a) and (1b) are real, while  $*$  stands for the complex conjugate.

Note that, rescaling the lattice fields  $u_n$  and  $v_n$  by a common factor, one can fix the value of  $\gamma_1$ , while  $\gamma_2$  remains an independent parameter. In this work, we use this option by fixing  $|\gamma_1| = 0.05$ . As for  $\gamma_2$ , we produce numerical results for  $\gamma_2 = \gamma_1$ , as variation of ratio  $\gamma_2/\gamma_1$  does not lead to a conspicuous change of the results. The sign of  $\gamma_{1,2}$  is essential, positive and negative ones representing, respectively, the self-focusing and defocusing  $\chi^{(3)}$  nonlinearity. In the absence of the  $\chi^{(2)}$  terms, this sign may be fixed by means of the *staggering transformation*,  $(u_n, v_n) \rightarrow (-1)^n (u_n, v_n)$  [20]. However, the present system does not admit it, as the sign of the  $\chi^{(2)}$  coefficient is already fixed. Below, we consider both signs of  $\gamma_{1,2}$ .

The FF lattice coupling constant in Eq. (1a) may be set to be positive,  $\epsilon > 0$  (if it is originally negative, its sign may be reversed by means of the complex conjugation of the equations). On the other hand,  $\delta > 0$  or  $\delta < 0$  in Eq. (1b) implies that the sign of the coupling constant in the SH subsystem is, respectively, opposite or identical to one for the FF wave, both cases being considered below. In the experiment, the magnitude and sign of the coupling constant in arrays of optical waveguides may be changed by means of the known diffraction-management scheme [18,19].

Stationary solutions to Eq. (1) are looked for as

$$u_n = e^{i\omega z} U_n, \quad v_n = e^{2i\omega z} V_n, \quad (2)$$

where real  $\omega$  is a propagation constant, and real discrete fields  $U_n, V_n$  satisfy the following equations:

$$(-\omega + \epsilon \Delta) U_n + U_n V_n + \gamma_1 (U_n^2 + 2V_n^2) U_n = 0, \quad (3a)$$

$$(q - 2\omega - \epsilon \delta \Delta) V_n + \frac{1}{2} U_n^2 + 2\gamma_2 (V_n^2 + 2U_n^2) V_n = 0. \quad (3b)$$

Linearizing these equations for the fields written in a formally complex form, it is straightforward to derive dispersion relations for the plane waves  $\sim \exp(ikn)$  in the FF and SH components:

$$\omega = -2\epsilon(1 - \cos k), \quad \omega = \epsilon\delta(1 - \cos k) + q/2, \quad (4)$$

where  $k$  is the spatial wavenumber. As it follows from Eq. (4), the propagation band for the plane waves in the FF component is

$$-4\epsilon < \omega < 0, \quad (5)$$

while for the SH component it is

$$q/2 < \omega < q/2 + 2\epsilon\delta \text{ for } \delta > 0, \quad (6)$$

$$q/2 - 2|\delta|\epsilon < \omega < q/2 \text{ for } \delta < 0. \quad (7)$$

Spectral intervals not covered by the propagation bands are considered as gaps. Thus, each band given by Eqs. (5) and (6), (7) is located between two semi-infinite gaps for the FF and SH components, respectively. The gaps extending to  $\omega \rightarrow +\infty$  and  $-\infty$  may host, severally, discrete solitons of the unstaggered and staggered types, the latter one assuming the structure of the lattice fields  $\sim (-1)^n$  [20]. To look for DE solutions, we assume that the FF propagation constant belongs to the semi-infinite gap corresponding to unstaggered discrete solitons, i.e.,  $\omega > 0$ , as it follows from Eq. (5). Simultaneously, it is assumed that the SH propagation constant,  $2\omega$ , falls into the corresponding propagation band given by Eqs. (6) or (7) (otherwise, one would be dealing with regular discrete solitons, rather than DEs).

### 3. Analytical approximations

#### 3.1. The continuum limit ( $\epsilon \gg 1$ )

For  $\epsilon \gg 1$ , Eqs. (3a) and (3b) may be approximated by their continuous counterparts:

$$-\omega U + U_{xx} + UV + \gamma_1(U^2 + 2V^2)U = -\frac{1}{12\epsilon}U_{xxxx} + \mathcal{O}(1/\epsilon^2), \quad (8a)$$

$$\begin{aligned} -2\omega V - \delta V_{xx} + qV + \frac{1}{2}U^2 + 2\gamma_2(V^2 + 2U^2)V_n \\ = -\frac{1}{12\epsilon}V_{xxxx} + \mathcal{O}(1/\epsilon^2). \end{aligned} \quad (8b)$$

In this limit (if the fourth derivatives may be omitted), and under the assumption that the SH component is much weaker than the FF one, i.e.,  $|V|^2 \ll |U|^2$ , Eqs. (3a), (3b) give rise to a known single-humped embedded-soliton solution [9].

The variational approximation, which may be efficiently used to construct soliton-like solutions of discrete equations [22–24], does not apply to Eqs. (3a), (3b), as well as to their continuous-limit counterparts (8a), (8b), because these systems cannot be derived from Lagrangians, except for the case of  $\gamma_1 = 2\gamma_2$  (numerical results are produced below for the case of  $\gamma_1 = \gamma_2$ , when the Lagrangian representation is not available). Nevertheless, it is possible to apply the averaging method [21], which uses an adopted ansatz, such as the one introduced below in Eq. (9), as an “optimal” approximate localized solution of Eqs. (3a), (3b). The averaging method amounts to the variational one if the underlying equation is Lagrangian [21].

Motivated by the example of the exact embedded soliton found in Ref. [9], we assume that localized solutions of Eqs. (8a) and (8b) may be approximated by

$$U = A \operatorname{sech}(\sqrt{\omega}x), \quad V = B \operatorname{sech}^2(\sqrt{\omega}x). \quad (9)$$

Following the averaging method, we substitute the ansatz in Eqs. (8a), (8b), multiply the first equation by  $\partial U/\partial A$  and the second one by  $\partial V/\partial B$ , and integrate the resulting expressions over  $-\infty < x < +\infty$ , to derive the following relations between parameters of the ansatz:

$$A^2 = \frac{1}{\gamma_1} \left( 2\omega - \frac{8}{5}B^2\gamma_1 - B - \frac{7\omega^2}{120\epsilon} \right), \quad (10a)$$

$$A^2 = \frac{2B[42(2\delta - 5)\omega - 144B^2\gamma_2 - 105q - 20\epsilon^{-1}\omega^2]}{21(32B\gamma_2 + 5)}. \quad (10b)$$

Approximate solutions given by Eqs. (10a), (10b) are candidates for embedded solitons in the case of  $\delta > 0$ . However, they do not select true DESs, as the actual SH component would likely include tails which do not vanish at  $x \rightarrow \pm\infty$ . We therefore need to impose an additional condition, which is the orthogonality of the localized solution (9) to the tail [25,26].

Because of the possible presence of the nonvanishing tail in the SH component, we seek for solutions in the form of

$$V = V_0 + CV_1, \quad (11)$$

where  $V_0$  is approximated by Eq. (9),  $C$  is a constant, and the asymptotic form of the tail has the form of  $V_1 \sim e^{\pm ikx}$  at  $x \rightarrow \pm\infty$ , where wavenumber  $k$  is given by dispersion relation following from the linearization of Eq. (8b), i.e.,

$$k^2 = 6\epsilon \left( -\delta \pm \sqrt{\delta^2 + (2\omega - q)/3\epsilon} \right). \quad (12)$$

Making use of the averaging method once again, we multiply Eq. (8b) by  $\partial V/\partial C$ , substitute  $C = 0$  in the resulting expression

(as we want to identify a DES), and integrate the equation over  $-\infty < x < +\infty$ , to derive the orthogonality condition

$$J \equiv \int_{-\infty}^{+\infty} N(U_0, V_0) \cos(kx) dx = 0, \quad (13)$$

where  $U_0$  is ansatz (9) for the approximate localized solution, and

$$\begin{aligned} N(U, V) = -2\omega V - \delta V_{xx} + qV + (1/2)U^2 + 2\gamma_2(V^2 + 2U^2)V_n \\ + (12\epsilon)^{-1}V_{xxxx}. \end{aligned} \quad (14)$$

The integral in Eq. (13) can be evaluated by means of residues of the analytically continued integrand,

$$\int_{-\infty}^{+\infty} N(V_0) \cos(kx) dx = -2\pi \sum \operatorname{Im} \operatorname{Res}[N(V_0)e^{ikx}], \quad (15)$$

where the summation is to be performed over all poles that lie in the upper complex half-plane of  $x$ . The analytical function written in Eq. (9) has infinitely many poles at imaginary values of the integration variable,  $x = (1 + 2n)i\pi/\sqrt{\omega}$ ,  $n = 0, 1, 2, \dots$ . However, the asymptotic limit is determined solely by the contribution from the lowest pole with  $n = 0$ , which yields

$$\begin{aligned} J \approx -\frac{2k\pi}{3\omega^3} \exp\left(\frac{k\pi}{2\sqrt{\omega}}\right) \times \left[ \frac{\gamma_2}{20}(k^2 + 4\omega)(k^2 + 16\omega)B^3 + \frac{3}{2}A^2\omega^2 \right. \\ \left. + 2\omega^2B\left(-3\omega + \left(4A^2\gamma_2 + \frac{3}{2}\delta k^2 + \frac{3}{2}q\right) + \frac{1}{\omega}A^2k^2\gamma_2 + \frac{1}{8\epsilon}k^4\right) \right]. \end{aligned} \quad (16)$$

Thus, Eqs. (10a), (10b), (12) and (16) predict values of parameters for DESs in the continuum limit,  $\epsilon \gg 1$ .

#### 3.2. The anti-continuum limit ( $\epsilon \ll 1$ )

In the anti-continuum limit, weakly coupled solutions of Eqs. (3a), (3b) may be approximated by the simplest ansatz [22],

$$U_n = A \exp(-\alpha|n|), \quad V_n = B \exp(-2\alpha|n|), \quad (17)$$

where amplitudes  $A$  and  $B$  are free parameters, and  $\alpha$  is determined by the condition that the ansatz must agree with a solution of the linearized version of Eq. (3a) for the tail of the FF component [25], i.e., with the first equation of system (4), in which  $\alpha = ik$  is substituted:

$$\alpha = \operatorname{arccosh}(1 + \omega/2\epsilon). \quad (18)$$

Next, we determine values of  $A$  and  $B$  in ansatz (17), again using the averaging method: the ansatz is substituted in Eqs. (3a), (3b), multiplying the first equation by  $\partial U_n/\partial A$ , the second one by  $\partial V_n/\partial B$ , and performing the summation over  $-\infty < n < +\infty$ , to obtain

$$(A^2\gamma_1 + B)F_4 + B^2\gamma_1F_6 + \epsilon e^{-\alpha} - \omega/2 - \epsilon = 0, \quad (19a)$$

$$\left( q - 2\omega + \frac{A^2}{2B} \right) F_4 + 2B^2\gamma_2F_8 + 4A^2\gamma_2F_6 + \frac{2\epsilon\delta}{F_2} = 0, \quad (19b)$$

where  $F_n \equiv \coth(n\alpha/2)$ .

Alternatively, the value of  $B$  may also be approximated by demanding that, if the ansatz is inserted in Eq. (3b), the tail of the SH component must be “locked” to the squared FF tail at  $|n| \rightarrow \infty$  (i.e., the tails of both components must jointly solve the asymptotic form of the equation):

$$B \approx A^2[\omega - q/2 + \epsilon\delta(\cosh(2\alpha) - 1)]^{-1}. \quad (20)$$

However, the latter approximation overestimates the role of the DES’ tails in comparison to its core region, which limits the applicability of the approximation, therefore we do not employ it here.

Similar to the situation considered above, Eqs. (19a) and (19b) do not select true DESs, while the appropriate selection is provided by the condition of the orthogonality of the soliton ansatz to the nonvanishing tail. To this end, the ansatz Eq. (17) including the tail is modified as  $V_n = B \exp(-2\alpha|n|) + \tilde{C}\tilde{V}_n$ , where  $C$  is a constant,  $\tilde{V}_n \sim \cos(nk)$  as  $n \rightarrow \pm\infty$ , and  $k$  is determined by the second equation of the system of dispersion relations (4), cf. Eq. (11). Also similar to what was done above, the orthogonality condition is obtained by multiplying expression (3b) by  $\tilde{V}_n$  and performing the summation over  $n$ :

$$J = \sum_{n=-\infty}^{+\infty} \cos(kn) \times \left[ (q - 2\omega - \epsilon \delta \Delta) V_n + \frac{1}{2} U_n^2 + 2\gamma_2 (V_n^2 + 2U_n^2) V_n \right] = 0. \tag{21}$$

The infinite sum in Eq. (21) can be calculated by means of the following formula:

$$\sum_{n=-\infty}^{+\infty} \cos(kn) e^{-aj|n|} \equiv \text{Re} \left\{ \sum_{n=-\infty}^{+\infty} e^{-aj|n|+ik|n|} \right\} = G_j, \tag{22}$$

where  $G_j = \sinh(j\alpha) / [\cosh(j\alpha) - \cos(k)e^{-j\alpha}]$ . Thus, Eq. (21) gives rise to the following selection condition for DES:

$$J = [2B\delta\epsilon(1 - \cos k) - 2\omega B + qB + A^2/2]G_2 + 2B^3\gamma_2G_6 + 4A^2B\gamma_2G_4 = 0. \tag{23}$$

The form of Eq. (23) clearly demonstrates that that this condition may be satisfied *only* in the case of the combined  $\chi^{(2)} : \chi^{(3)}$  nonlinearity: if the cubic terms are absent, i.e.,  $\gamma_2 = 0$ , Eq. (23) cannot hold.

Thus, Eqs. (19a), (19b) and (23) predict parameter values for DESs in the anti-continuum limit,  $|\epsilon| \ll 1$ .

#### 4. Numerical results

The numerical solution of stationary Eqs. (3a) and (3b) was obtained by employing an iterative optimization algorithm for the solution of nonlinear least-squares problems through the function `fsolve` of MATLAB. Once DES components  $U_n$  and  $V_n$  had been found, we studied stability of the solution by substituting a perturbed solution,  $u_n = (U_n + (\hat{r}_n + i\tilde{r}_n)e^{\lambda z} + (\hat{r}_n^* + i\tilde{r}_n^*)e^{\lambda^*z})e^{i\omega z}$  and  $v_n = (V_n + (\hat{s}_n + i\tilde{s}_n)e^{\lambda z} + (\hat{s}_n^* + i\tilde{s}_n^*)e^{\lambda^*z})e^{2i\omega z}$  into Eqs. (1a), (1b) and linearizing them with respect to small perturbations  $\hat{r}_n, \tilde{r}_n, \hat{s}_n$  and  $\tilde{s}_n$ , arriving at the following problem for stability eigenvalue  $\lambda$ :

$$-\lambda D \begin{pmatrix} \hat{r}_n \\ \tilde{r}_n \\ \hat{s}_n \\ \tilde{s}_n \end{pmatrix} = \begin{pmatrix} 0 & L_{1,-} & 0 & U_n \\ L_{1,+} & 0 & U_n + 4\gamma_1 U_n V_n & 0 \\ 0 & U_n & 0 & L_{2,-} \\ U_n + 8\gamma_2 U_n V_n & 0 & L_{2,+} & 0 \end{pmatrix} \begin{pmatrix} \hat{r}_n \\ \tilde{r}_n \\ \hat{s}_n \\ \tilde{s}_n \end{pmatrix}, \tag{24}$$

where we have defined a diagonal matrix,

$$D \equiv \begin{pmatrix} 1 & 0 & 0 & 0 \\ 0 & -1 & 0 & 0 \\ 0 & 0 & 1 & 0 \\ 0 & 0 & 0 & -1 \end{pmatrix},$$

and linearisation operators

$$L_{1,\mp} = \epsilon \Delta - \omega \mp V_n + \gamma_1 ((2 \mp 1)U_n^2 + 2V_n^2),$$

$$L_{2,\mp} = -\epsilon \delta \Delta - \omega + q + 2\gamma_2 ((2 \mp 1)V_n^2 + 2U_n^2).$$

DES is unstable when there are eigenvalues  $\lambda$  with nonzero real parts, and linearly stable otherwise. A semi-analytical approximation for identifying critical eigenvalues by means of the variational formulation is possible (see, e.g., Ref. [27] and references therein), but we do not pursue this direction here.

After identifying the (in)stability of DES in terms of the eigenvalues, their perturbed evolution was investigated, simulating Eqs. (1a) and (1b) by means of the fourth-order Runge-Kutta method in the temporal direction.

#### 4.1. Broad discrete embedded solitons

First, in Fig. 1(a) we display an example of a numerically found DES, obtained in the lattice built of  $N = 100$  sites, and its counterpart, produced by means of the approximation based on Eqs. (9), (10a), (10b), (13), and (12), (16), for values of parameters in Eqs. (1a), (1b)  $\epsilon = 10, q = 1, \gamma_1 = \gamma_2 = -0.05$  (recall that  $\gamma_{1,2} < 0$  implies the defocusing sign of the  $\chi^{(3)}$  nonlinearity) and propagation constant  $\omega = 0.7$ . Because DES is a solution of the codimension-one type, for these arbitrarily chosen parameters the numerical solution can be found only for a specially selected value of the remaining one, viz., the relative strength of the lattice coupling for the SH wave,  $\delta \approx 0.9391$ , while the analytical approximation yields  $\delta \approx 0.8645$  [recall that  $\delta > 0$  implies opposite signs of the SH and FF lattice couplings in Eqs. (1a) and (1b)]. At these values of the parameters, the gap in the linear spectrum of the SH component, as given by Eq. (6), is  $0.5 < \omega < 19.3$ , hence  $\omega = 0.7$  indeed belongs to the band (sitting close to its edge), confirming that the discrete soliton is of the embedded type.

The use of the above approximation, corresponding to the continuum limit, is relevant here, as  $\epsilon = 10$  is large enough for this purpose. Note also that the relatively small value of the propagation constant,  $\omega = 0.7$ , makes the DES broad enough [as per Eq. (9)], which additionally justifies the use of the quasi-continuum formalism in this case. It is remarkable that the analytical approximation produces a virtually exact DES solution in Fig. 1(a).

Fixing parameters  $q = 1$  and  $\gamma_{1,2} = -0.05$ , and propagation constant  $\omega = 0.7$  as above, the variation of  $\epsilon$  makes it possible to produce two branches of numerical solutions of Eqs. (3a), (3b) in the  $(\epsilon, \delta)$  plane, as shown in Fig. 1(b) by the solid curve with a turning point at  $\epsilon = \epsilon_{\min} \approx 2.14$ , at which the two branches merge. Thus, Fig. 1(b) shows that the continuation of the DES families does not exist if the coupling constant falls below the minimum value. Note that, for the currently fixed values,  $q = 1$  and  $\omega = 0.7$ , the SH band, given by Eq. (6), amounts to  $\epsilon\delta > 0.1$ . Obviously, the entire solid curve in Fig. 1(b) belongs to this area. It is also worthy to note that both branches exist at  $\delta > \delta_{\min} \approx 0.36$  [in particular, DESs do not exist at  $\delta < 0$ , when the coupling constants in the FF and SH sublattices have the same signs, see Eqs. (1a) and (1b)].

The analytical approximation based on Eqs. (9), (10a), (10b), (13), and (16) produces a single existence branch, shown by the dashed line in Fig. 1(b), which cannot be extended beyond the left end point, i.e., the approximation predicts, in a qualitatively correct form, only one branch of the DES solutions. We assume that this happens because ansatz (9) is not sufficiently versatile to capture the other branch of the solutions. A better ansatz may be tried, but it would lead to an extremely cumbersome analysis.

#### 4.2. Narrow discrete embedded solitons

The above results were obtained for a situation close to the continuum limit. Fig. 2 presents typical findings for the opposite case, close to the anti-continuum limit, in the lattice composed of  $N = 30$  sites. First, an example of a strongly discrete embedded soliton is displayed in panel (a) for parameters of Eqs. (1a) and

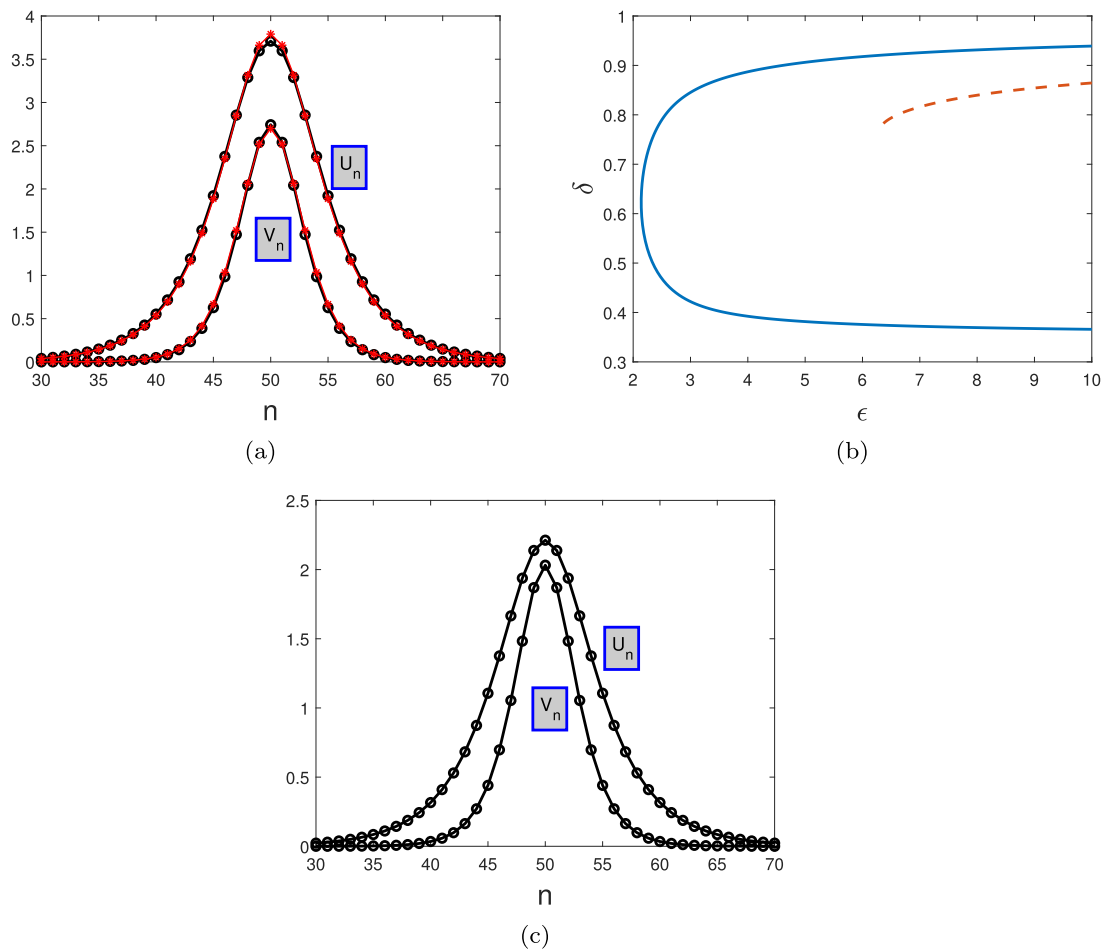


**Fig. 1.** (a) A discrete embedded soliton (DES) for parameters of Eqs. (1a) and (1b)  $\epsilon = 10$ ,  $q = 1$ ,  $\omega = 0.7$ ,  $\gamma_1 = \gamma_2 = -0.05$ ,  $\delta \approx 0.9391$ , and propagation constant  $\omega = 0.7$  [see Eq. (2)]. Circles and stars depict, severally, a numerical solution of Eqs. (3a), (3b), and its counterpart produced by the analytical approximation, based on Eqs. (9), (10a), (10b), (13), and (12), (16). The location of DES according to our approximation is at  $\delta \approx 0.8645$ . (b) A solid curve in the plane of  $(\epsilon, \delta)$ , along which the numerical solution produces DES states, with other parameters fixed at the same values as in panel (a). The dashed curve shows a similar result produced by the analytical approximation. (c) A numerically found DES solution belonging to the lower branch in panel (b), for the same parameters as in (a), except for  $\delta \approx 0.3659$ . In panels (a) and (c), taller and lower profiles represent the FF and SH fields, i.e.,  $U_n$  and  $V_n$ , respectively. DES families represented in this figure are completely unstable. see Fig. 3 below.

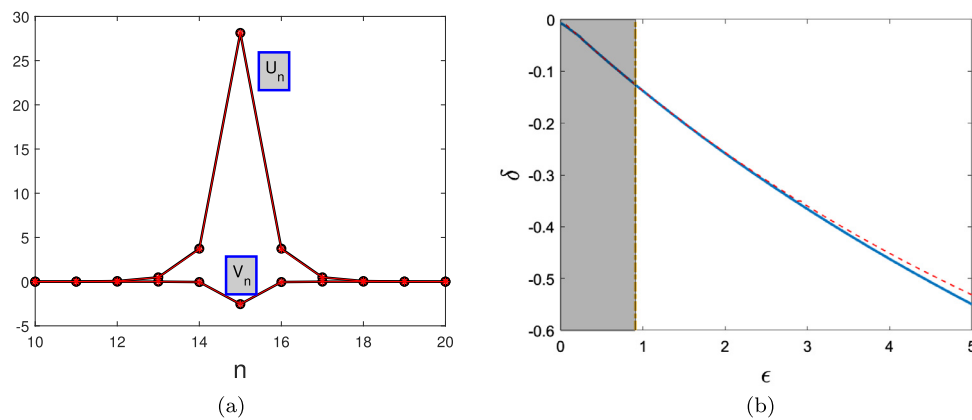


**Fig. 2.** The same as Fig. 1(a,b), but for the weakly coupled lattice with parameters  $q = 60$ ,  $\gamma_1 = \gamma_2 = 0.05$ , and propagation constant  $\omega = 29$ . In panel (a),  $\epsilon = 5$  and  $\delta \approx -0.5496$ . The FF and SH profiles,  $U_n$  and  $V_n$ , are positive and negative ones. This DES is a completely stable one, see Fig. 5 below. The shaded region in panel (b) shows the domain of existence of regular (non-embedded) solitons.

(1b) chosen as  $\epsilon = 5$ ,  $q = 60$ ,  $\gamma_1 = \gamma_2 = 0.05$ , and propagation constant  $\omega = 29$ , while the value of coefficient  $\delta$ , at which the non-generic DES is found numerically, is  $\delta \approx -0.5496$ . Note that the negative sign of  $\delta$  implies identical signs of the inter-site coupling in the FF and SH sublattices, on the contrary to the case displayed

above in Fig. 1. At these values of the parameters, the SH band, defined by Eq. (7), is  $24.5 < \omega < 30$ , to which  $\omega = 29$  indeed belongs, sitting close to its edge.

The analytical approximation for the strongly discrete DES, based on Eqs. (17), (18), and (23) is also displayed, for the same

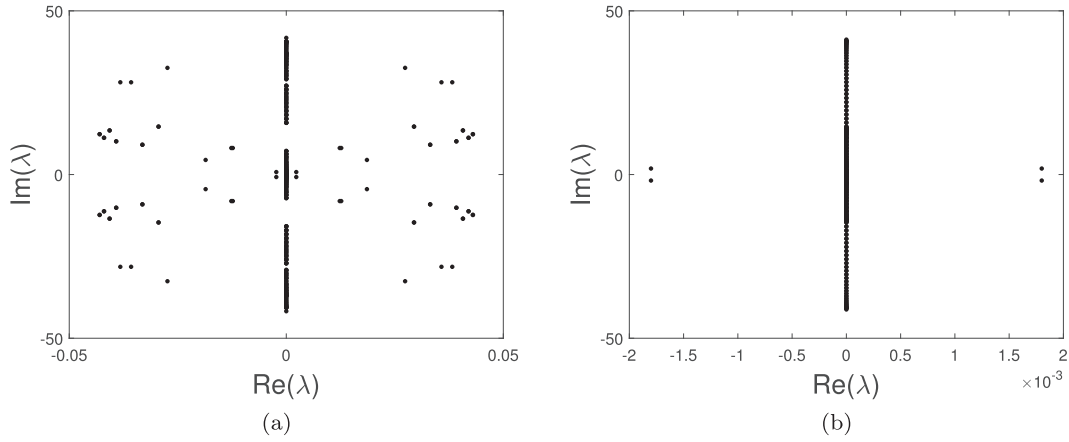


Fig. 3. Panels (a) and (b) show spectra of complex stability eigenvalues for DES displayed in Fig. 1a and c, respectively.

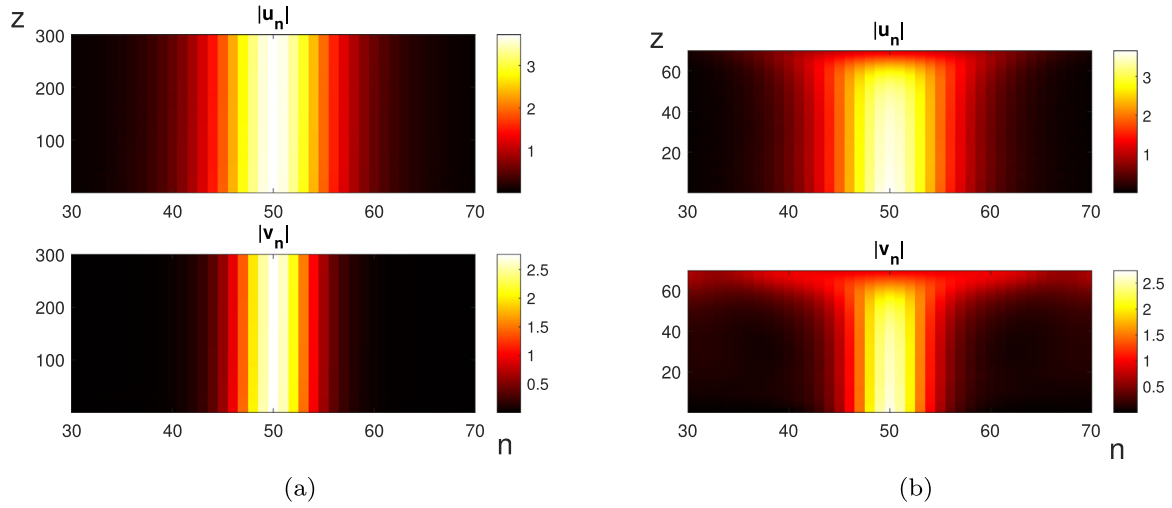


Fig. 4. The evolution of DES from Fig. 1(a) under the action of complex random-noise perturbations with maximum modulus amplitude  $2 \times 10^{-2}$ ; and (b) after being initially perturbed by rescaling its shape, according to  $u_n(t = 0) = 0.99 \times U_n$ ,  $v_n(t = 0) = 0.99 \times V_n$ .

parameters, in Fig. 2(a). It is seen to be virtually identical to the numerical counterpart.

In a still simpler approximation, which may be applied to a strongly discrete soliton, its FF and SH amplitudes,  $U_0$  and  $V_0$ , can be found by completely neglecting the coupling of the central site,  $n = 0$ , to the adjacent ones,  $n = \pm 1$  [28]. In this limit, Eqs. (3a), (3b) yield, in the expectation of having  $U_0^2 \gg V_0^2$ , the following values:

$$V_0 \approx -1/(8\gamma_2) = -2.5, U_0 \approx \sqrt{(\omega - V_0)/\gamma_1} \approx 25.1, \quad (25)$$

which are close enough to ones observed in Fig. 2(a).

A family of DES modes, produced by the numerical solution of Eqs. (3a), (3b) for the same parameters as in Fig. 2(a), i.e.,  $q = 60$ ,  $\gamma_{1,2} = 0.05$ , and  $\omega = 29$ , but with a varying coupling constant  $\epsilon$ , and  $\delta$  adjusted accordingly, is displayed in Fig. 2(b), along with its counterpart produced by the above-mentioned analytical approximation, based on Eqs. (17), (18), and (23). It is clearly seen that the approximation is very accurate in this case, even for relatively large values of  $\epsilon$ , for which the applicability of the anti-continuum formalism is not evident. Unlike the family shown above in Fig. 1, with identical signs of the FF and SH components, the present one always features opposite signs.

Lastly, we note that, for the parameters chosen in Fig. 2(b), Eq. (7) defines the SH band as the area with  $|\delta|\epsilon > 0.5$ . This condition means that the family presented in this figure belongs to the band at  $\epsilon > \epsilon_0 \approx 0.9098$ , while its extension to  $\epsilon < \epsilon_0$  immerses

into the bandgap, as a family of regular solitons (non-embedded ones). In the figure, the existence region of the regular solitons is shaded.

### 4.3. Stability and evolution of discrete embedded solitons

We address the stability of DESs by numerically solving the eigenvalue problem (24). First, we consider the case of opposite signs of the coupling constant in the SH and FF lattices, i.e.,  $\delta > 0$  in Eq. (1b). The first result is that the solution branches in Fig. 1b are completely unstable. As an illustration, the spectrum of the eigenvalues displayed in Fig. 1a and b is shown in Fig. 3. In these cases, the oscillatory instability is accounted for by quartets of complex eigenvalues.

Having established the instability of the DESs shown in Fig. 1a, we display simulations of their dynamics, under the action of two different perturbations, in Fig. 4. First, Fig. 4a demonstrates that the soliton, in spite of the presence of many unstable eigenvalues in its perturbation spectrum, as seen in Fig. 3a, is actually quite robust in direct simulations which include small random perturbations in the initial conditions. In this connection, we note that, with  $\epsilon = 10$  and  $\delta$  close to 1 (the values used in Fig. 1), and the soliton's width  $W \sim 10$  (as seen in the same figure), the characteristic diffraction (Rayleigh) length is  $Z_{\text{diff}} \sim W^2/\epsilon \sim 10$ , i.e., the total propagation distance displayed in Fig. 4(a) is  $\sim 30$  diffraction lengths, which is actually a very large value in a real experiment

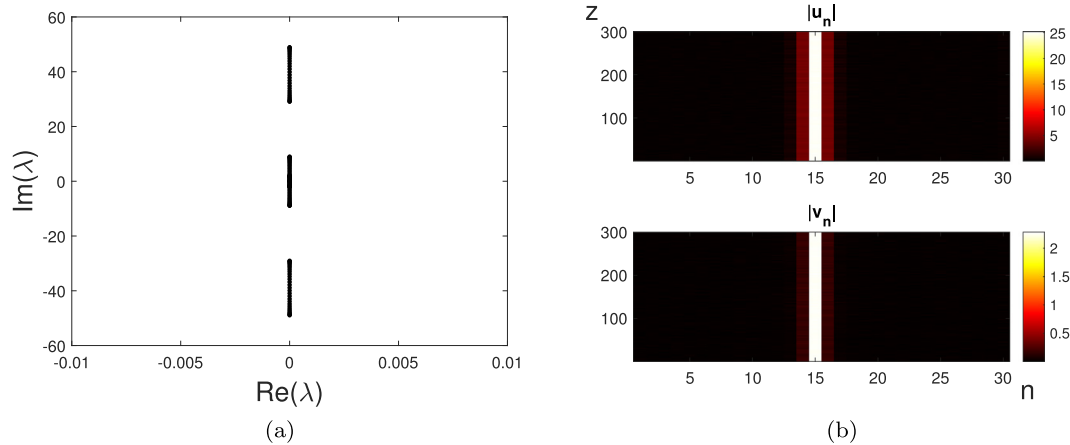


**Fig. 5.** (a) The spectrum of perturbation eigenvalues for the DES from Fig. 2a. (b) The simulated evolution of the same soliton, with an initial perturbation in the form of  $u_n(t=0) = 0.9 \times U_n$ ,  $v_n(t=0) = 0.9 \times V_n$ . This, relatively strong, perturbation leaves the soliton completely stable, unlike a much weaker initial scaling perturbation which destroys the DES in Fig. 4(b).

[3–6]. On the other hand, if the initial state is perturbed merely by multiplying it by factor 0.99, the DES originally stays nearly intact, over the distance  $Z \simeq 60 \sim 6Z_{\text{diff}}$ , and then quickly decays, as shown in Fig. 4b. The latter dynamical scenario is typical for the “one-sided” semistability of embedded solitons [9], initiated by slow sub-exponential growth of perturbations, which eventually leads to fast destruction of the solitons. The perturbed evolution of the DES displayed in Fig. 1c exhibits similar dynamical behavior (not shown here in detail).

Next, we consider the case of  $\delta < 0$ , i.e., opposite signs of the intersite linear couplings in the FF and SH lattices in Eqs. (1a) and (1b). For the DES shown in Fig. 2a, its linear-perturbation spectrum is plotted in Fig. 5a, which does not include unstable eigenvalues (the spectrum is purely imaginary). This is the case with all DESs along the existence curve plotted in Fig. 2b. Direct simulations of the evolution of the soliton subjected to the scaling perturbation, similar to that which led to the destruction of the semistable soliton in Fig. 4(b), but actually much stronger (with the initial scaling factor 0.9 instead of 0.99), demonstrate perfect stability. Under the action of random perturbations, the same soliton is perfectly stable as well (not shown here in detail). Thus, the system of Eqs. (1a) and (1b) with  $\delta < 0$  produces fully stable DESs, which were not reported before.

## 5. Conclusion

In this work, we have revisited the problem of the creation of DESs (discrete embedded solitons) in the model of the light propagation in an array of tunnel-coupled waveguides with the combined on-site quadratic and cubic nonlinearities. Two analytical approximations have been developed, based on the averaging method, which apply, severally, to broad and narrow DESs. Systematic results are obtained by means of numerical calculations. Both analytical and numerical methods produce DESs of different types – in particular, with identical or opposite signs of the FF (fundamental-frequency) and SH (second-harmonic) components. The analytical approximation yields very accurate results, in comparison to their numerically found counterparts, for the most interesting case of strongly discrete embedded solitons. In that case, the DES family crosses the border of the spectral propagation band and extends, as a branch of regular solitons, into the semi-infinite gap. The analytical approximations developed here for the DESs may be applied to other physically relevant discrete models. Stability of the DESs has been investigated numerically. While it is generally known that DESs are semi-stable objects, which we ob-

served as well here, in the case of FF and SH components having intersite coupling coefficients with opposite signs, we demonstrate the existence of remarkably stable DESs, which, to the best of our knowledge, has not been reported before.

A challenging direction for the development of the present analysis is to perform it for two-dimensional lattices with the  $\chi^{(2)} : \chi^{(3)}$  nonlinearity, with the aim to seek for two-dimensional DESs.

## Declaration of Competing Interest

The authors declare that they have no known competing financial interests or personal relationships that could have appeared to influence the work reported in this paper.

## CRediT authorship contribution statement

**Hadi Susanto:** Conceptualization, Methodology, Formal analysis, Investigation, Writing – original draft, Visualization. **Boris A. Malomed:** Conceptualization, Methodology, Writing – review & editing.

## Acknowledgements

HS thanks Mahdhivan Syafwan for fruitful discussions at the early stage of this work. The work of BAM is supported, in part, by Israel Science Foundation through grant No. 1286/17. This author appreciates hospitality of Department of Mathematical Sciences at the University of Essex (UK).

## References

- [1] Shen YR. The principles of nonlinear optics. New York: Wiley; 1984.
- [2] Karamzin YN, Sukhorukov AP. Nonlinear interaction of diffracted light beams in a medium with quadratic nonlinearity – mutual focusing of beams and limitation on efficiency of optical frequency converters. Pisma Zh Exp Teor Fiz 1974;20:730. [JETP Lett 1975;20:338]
- [3] Torruellas WE, Wang Z, Hagan DJ, van Stryland EW, Stegeman GI, Torner L, Menyuk CR. Observation of 2-dimensional spatial solitary waves in quadratic medium. Phys Rev Lett 1995;74:5036.
- [4] Stegeman GI, Hagan DJ, Torner L.  $\chi^{(2)}$  cascading phenomena and their applications to all-optical signal processing, mode-locking, pulse compression and solitons. Opt Quantum Electron 1996;28:1691–740.
- [5] Etrich C, Lederer F, Malomed BA, Peschel T, Peschel U. Optical solitons in media with a quadratic nonlinearity. Prog Opt 2000;41:483–568.
- [6] Buryak AV, Tripani PD, Skryabin DV, Trillo S. Optical solitons due to quadratic nonlinearities: from basic physics to futuristic applications. Phys Rep 2002;370:63–235.

- [7] Karpierz MA. Coupled solitons in waveguides with second- and third-order nonlinearities. *Opt Lett* 1995;20:1677–9.
- [8] Buryak AV, Kivshar YS, Trillo S. Optical solitons supported by competing nonlinearities. *Opt Lett* 1995;20:1961–3.
- [9] Yang J, Malomed BA, Kaup DJ. Embedded solitons in second-harmonic-generating systems. *Phys Rev Lett* 1999;83:1958–61.
- [10] Champneys AR, Groves MD. A global investigation of solitary waves solutions to a two-parameter model for water waves. *J Fluid Mech* 1997;342:199–229.
- [11] Fujioka J, Espinosa A. Soliton-like solution of an extended NLS equation existing in resonance with linear dispersive waves. *J Phys Soc Jpn* 1997;66:2601–7.
- [12] Champneys AR, Malomed BA, Yang J, Kaup DJ. “Embedded solitons”: solitary waves in resonance with the linear spectrum. *Physica D* 2001;152–153:340–54.
- [13] Haller G. A variational theory of hyperbolic lagrangian coherent structures. *Physica D* 2011;240:574–98.
- [14] Yang JK. Stable embedded solitons. *Phys Rev Lett* 2003;91:143903.
- [15] Iwanow R, Schiek R, Stegeman GI, Pertsch T, Lederer F, Min Y, Sohler W. Observation of discrete quadratic solitons. *Phys Rev Lett* 2004;93:113902.
- [16] Lederer F, Stegeman GI, Christodoulides DN, Christodoulides DN, Assanto G, Segev M, Silberberg Y. Discrete solitons in optics. *Phys Rep* 2008;463:1–126.
- [17] Yagasaki K, Champneys AR, Malomed BA. Discrete embedded solitons. *Nonlinearity* 2005;18:2591–613.
- [18] Eisenberg HS, Silberberg Y, Morandotti R, Boyd A, Aitchison JS. Diffraction management. *Phys Rev Lett* 2000;85:1863–6.
- [19] Pertsch T, Silberberg Y, Peschel U, Lederer F. Anomalous refraction and diffraction in discrete optical systems. *Phys Rev Lett* 2002;88:093901.
- [20] Cai D, Bishop AR, Grønbech-Jensen N. Localized states in discrete nonlinear Schrödinger equations. *Phys Rev Lett* 1994;72:591–5.
- [21] Dawes JH, Susanto H. Variational approximation and the use of collective coordinates. *Phys Rev E* 2013;87:063202.
- [22] Malomed BA, Weinstein MI. Soliton dynamics in the discrete nonlinear Schrödinger equation. *Phys Lett A* 1996;220:91–6.
- [23] Kaup DJ. Variational solutions for the discrete nonlinear Schrödinger equation. *Math Comp Simul* 2005;69:322–33.
- [24] Malomed BA, Kaup DJ, Gorder RAV. Unstaggered-staggered solitons in two-component discrete nonlinear Schrödinger lattices. *Phys Rev E* 2012;85:026604.
- [25] Kaup DJ, Malomed BA. Embedded solitons in lagrangian and semi-lagrangian systems. *Physica D* 2003;184:153–61.
- [26] Syafwan M, Susanto H, Cox SM, Malomed BA. Variational approximations for traveling solitons in a discrete nonlinear Schrödinger equation. *J Phys A* 2012;45(7):075207.
- [27] Rusin R, Kusdiantara R, Susanto H. Variational approximations using gaussian ansatz, false instability, and its remedy in nonlinear Schrödinger lattices. *J Phys A* 2018;51(47):475202.
- [28] Aubry S. Breathers in nonlinear lattices: existence, linear stability and quantization. *Physica D* 1997;103:201–50.